Electronic Supplementary Material (ESI) for Nanoscale.

Supplementary information

In this work two groups were studied: the first composed by 15 donor volunteers; the second by 5 diabetic subjects. 10 cells were measured for each of the subjects. Cells were chosen by using optical microscope images. The JPK AFM NanoWizardII used in this experiment is indeed coupled to an inverted optical microscope (Zeiss Axio Observer) that allows for the precise positioning of the AFM tip on the desired cells. The typical optical image showing both RBCs and the AFM tip is reported in fig S1. Fig. S1 shows the presence of three main different cell shapes: a major fraction of the typical biconcave red blood cells, and a minor fraction composed by flattened and thorny red blood cells. Only cells belonging to the first category were chosen for the present study.

We want to stress again that cells belonging to the second category are a minor fraction of the observed red blood cells. The high incidence of flat and thorny cells shown in fig s1 (lower panel) is thus not statistically representative of their occurrence in the sample investigated.

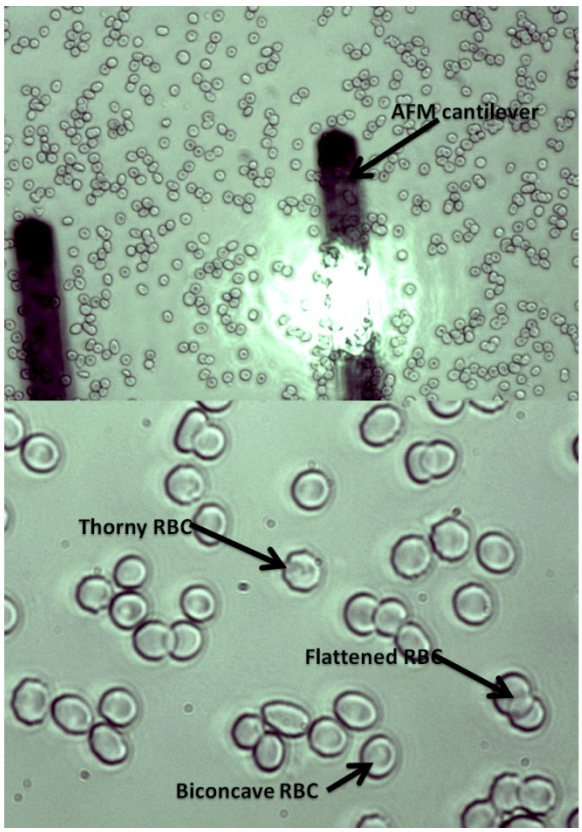

Fig. S1: Optical micrograph showing both the AFM tips and a typical field endowing some of the investigated cells (upper panel); an enlarged detail (lower panel) shows the presence of three different type of red blood cells.

As discussed in tab. S1 the measured RBC Young's modulus has a large dispersion due to the presence of a large biological variability, to the different clinical conditions of subjects and, not least, to the fact that sample preparation affects strongly the mechanical response of cells. In fig 1e (main text), we reported the spatial Young's modulus distribution measured for the typical RBC, i.e. characterized by a Young's modulus close to the average value measured over the whole group of healthy volunteers. In order to provide a more in-depth description, we reported the same nanoscale spatial distribution for a RBC characterized by an average Young's modulus significantly above (fig S2) and below (fig S3) the average Young's modulus computed for all the healthy subjects.

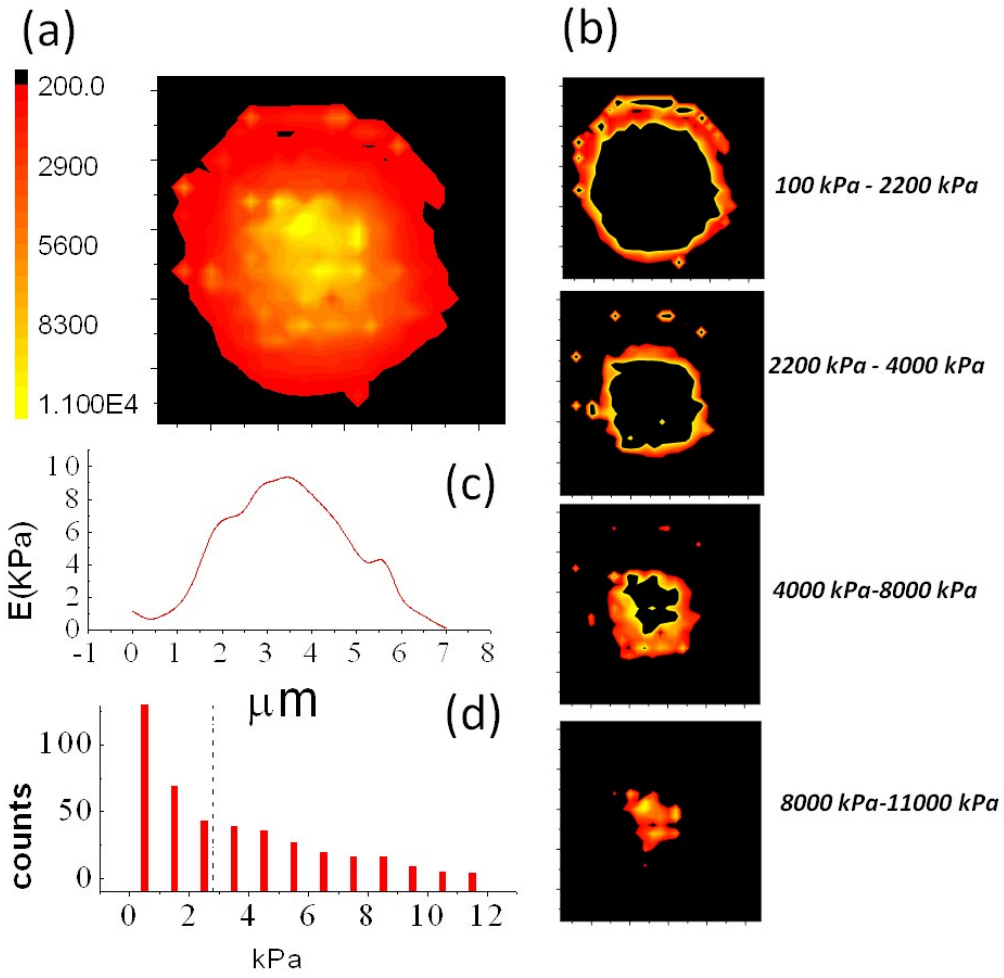

Fig. S2: local mechanical response of a red blood cell characterized by an average Young's modulus of about 2.8 kPa. (a) Young's modulus map of the red blood cells. The unit of the color scale-bar is Pascal. (b) Four "iso-elastic" maps showing only the E values comprised in a fixed range. (c) Typical Young's modulus profile acquired from fig S2a. (d) Histogram of the Young's modulus computed over the whole cell.

To make the Young's modulus spatial distribution more understandable we plotted in both cases four "iso-elastic" maps. In these maps, only values comprised in a defined range are represented,

whereas data out of this range are not visualized (panel b). Moreover, a typical line profile (panel c) and an histogram computed over the whole cell (panel d) were also shown. We feel that this kind of graphical representation helps to better clarify the Young's modulus distribution within the cell at the center and at the edge.

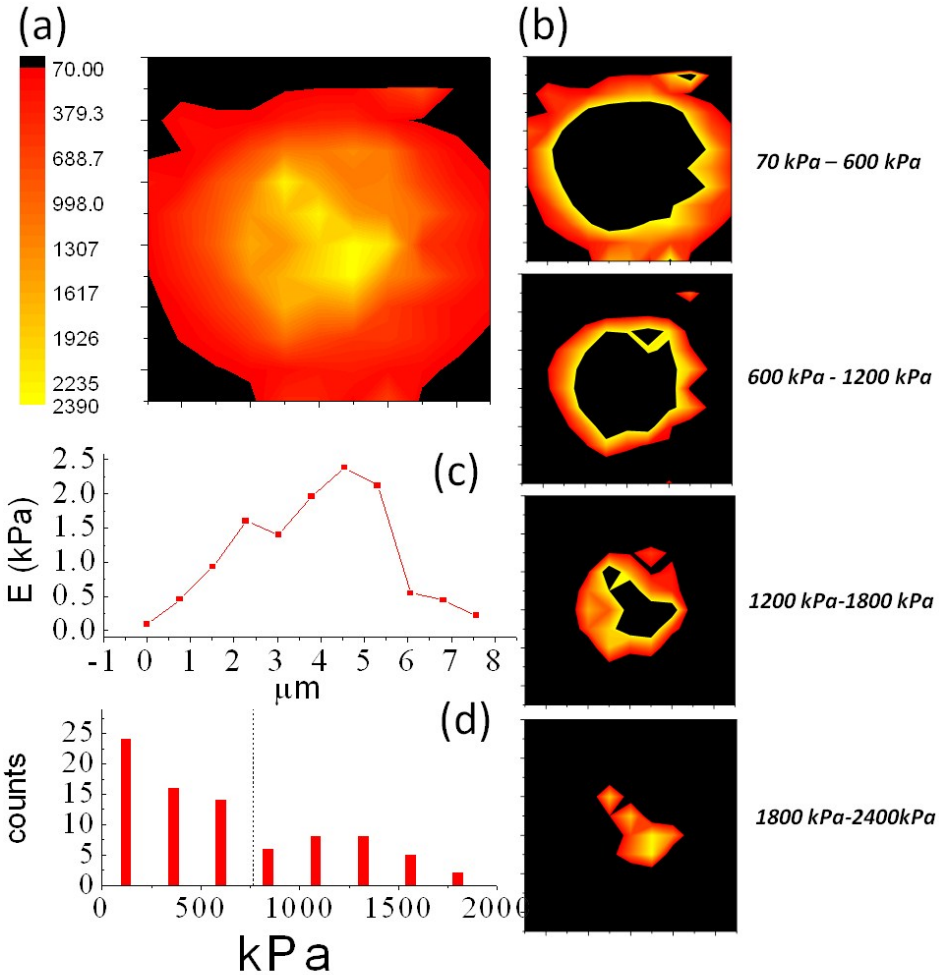

Fig. S3: local mechanical response of a red blood cell characterized by an average Young's modulus of about 0.5 kPa. (a) Young's modulus map of the red blood cells. The unit of the color scale-bar is Pascal. (b) four "iso-elastic" maps showing only the E values comprised in a fixed range. (c) Typical Young's modulus profile acquired from fig S2a. (d) Histogram of the Young's modulus computed over the whole cell.

Although the average Young's modulus may change for different red blood cells, as expected and as shown in fig 1, S2 and S3, the cylindrical distribution of E values shown in fig 1 is highly conserved over the measured cells irrespectively of the subjects and the average E value, confirming that the detected behavior is a general characteristic of red blood cells.

To provide a more direct comparison with other studies dealing with RBCs mechanical response we compare the main results of this paper with that shown in similar works. In particular, tab. S1 provides information on the numerosity of the sample studied, the average measured Young's module, its standard deviation and, when explicitly indicated, the indentation rate.

	Subjects	Average E (kPa)	Dispersion (kPa)	Rate	Preparation
Reference [4]	**N=13 healthy subjects**	**4.9±0.5**	**3.6±0.4**	**Not indicated**	**not fixed dried cells**
	Hospitalized subjects N=19 Diabetes Mellitus N=33 hypertension N=22 Coronary disease	**8.6±0.8**	**7.6±0.9**		
Reference [11]	**Healthy volunteers** (Number not reported)	Ranges between **75-115**	**Not indicated**	**Not indicated**	**Fixed cells**
Reference [8]	**Healthy volunteers** (Number not reported)	Ranges between **1.27-7.22**	**Not indicated**	Ranges between **0.6-2.8 μm/s**	**Not fixed cells resuspened in PBS solution**
Reference [10]	Healthy subjects (Number not reported)	26	7	Not indicated	**Fixed cells (0.5% glutaraldehyde) resuspended in PBS**
	Hereditary spherocitosys (Number not reported)	43	21		
	Thalassemia (Number not reported)	40	24		
	G6PD deficiency (Number not reported)	90	20		
Reference [13]	**Healthy subjects** (Number not reported)	Ranges between **0.1-0.2**	**Not indicated**	**Not indicated**	**Not fixed cells resuspended in Hank's balanced salt solution (HBSS).**
Reference [1]	**Healthy subjects** (Number not reported)	monomodal distribution peaked at **1.1 ±0.4**	**Not indicated**	**Not indicated**	**Unfixed cells resuspended in PBS solutions**
	Sickle cell disease (Number not reported)	binomodal distribution peaked at **1.1 ±0.4** and at **3.0±0.5**			
Reference [12]	**N=40 Healthy subjects**	**1.81±0.4**	**Not indicated**	**Not indicated**	**Unfixed dried cells**
Present paper	**N=15 Healthy subjects**	**1.82 ±0.20**	**1.6**	**5 μm/s**	**Unfixed cells resuspended in PBS solutions**
	N=5 Diabetes mellitus	**2.52±0.58**	**2.9**	**5 μm/s**	

Tab S1: comparison of the main results of the present paper to that shown in similar experimental works.

Table S1 shows that the average E value displays a large variability that goes behind the (still large) biological variability. Among the other causes, this additional source of variability appears to be dependent on the sample preparation protocol. It can be indeed noted that fixed cells are significantly stiffer than dried cells that, in their turn, are stiffer than not fixed cells in PBS. The average Young's modulus measured in the present paper appears to be consistent within the standard deviation with the values obtained by using similar sample preparation. Merit of note is the extremely low E value measured in ref [13], that could be dependent on the buffer solution used. This point is highly interesting and deserves a more in-depth study. On the other hand, an overall E value of about 200 Pa may be due to the presence of loosely attached cells.

A further source of variability may depend on the indentation rate used for the measurements. We indeed demonstrated that large variations (about 30%) might occur by increasing the indentation rate from few μm/s to few tents of μm/s. Since the indentation rate is generally not indicated, except in ref [8], this source of variability cannot be properly estimated.